

Alan Mannoosseril<sup>1</sup>, Sondipon Adhikari<sup>1</sup>, Alex P. Prado<sup>2</sup> & Pedro H. Cabral<sup>2</sup>

<sup>1</sup>James Watt School of Engineering, University of Glasgow, Glasgow G12 8QQ, Scotland, United Kingdom <sup>2</sup>Embraer S.A., São José dos Campos, Brazil

#### **Abstract**

This study tackles intrinsic uncertainties in aircraft constructions caused by complicated system characteristics and modelling complexities, frequently compounded by a lack of accurate knowledge. It presents an application of an uncertainty model based on random matrices and stochastic finite element analysis. In particular, the Wishart Random Matrix model quantifies uncertainty in critical structural components—mass, stiffness, and damping matrices—without comprehensive data. The approach, implemented through the NASTRAN framework, uses eigenvalues from free vibration analysis instead of extracting component matrices and introduces randomness using Monte Carlo Simulations to build probability distributions. Python integration with NASTRAN improves optimisation and usability. The study shows that the Wishart random matrix model and simplified matrix randomisation are useful for cost-efficient analysis of aerostructures. This paper expands the application of random-matrix-based uncertainty quantification to prestressed complex structures, which is particularly beneficial for large-scale structures such as aircraft. This methodology enhances design control in uncertainty modelling and propagation by providing flexibility in modifying dispersion levels and aligning with physical models.

Keywords: Uncertainty, Random Matrix, Eigenvalues, NASTRAN, Python

## 1. Introduction

Analysis of aircraft structures involves uncertainties arising from parameters and modelling of the complex system. However, in practical scenarios, information on these uncertainties is rarely available. Here, we utilise uncertainty models to represent these complex structural uncertainties in random matrices and stochastic finite element analysis.[1, 2, 3] In this paper, a practical application of the Wishart Random Matrix model is presented to quantify the total uncertainty in the random vibration frequency values of the model using diagonal eigenvalue matrix, without the use of stiffness, mass or damping matrices and also relying on Monte Carlo Simulations. This work addresses a new uncertainty quantification process in structural analysis utilising the NASTRAN framework instead of extracting the component matrices, using eigenvalues of free vibration analysis from the output, and employing randomness in the system to generate the probability distribution. Researchers may use MATLAB for finite element modelling, but the industry typically prefers commercial packages due to their graphical interfaces, open-sourced nature, and time efficiency. Therefore, this study utilises Python combined with NASTRAN to enhance optimisation and facilitate ease of use for large and complex structures. For similar Python-based work in structural dynamics see [4, 5]

Previous research has demonstrated that the Wishart random matrix model may be coupled with the reduced model decomposition technique to analyse stochastic built-up structures cost-effectively

when precise information about uncertainty is missing.[6] This paper scales the problem for a prestressed (when dealing with nonlinear material behaviour or geometric stress-stiffness) complex structure with multiple element types and a higher element number while discussing an analogous beam model for empirical understanding.

Random-matrix-based uncertainty quantification is more beneficial as it can be employed in systems with nominal information, benefiting large-scale complex structures like aircraft. Modelling system matrices as random matrices allows adjusting dispersion levels, aligning with physical models of structures for enhanced design freedom and control in uncertainty modelling and propagation.

## 2. Random matrix approach for stochastic dynamic analysis

# 2.1 Matrix Variate Probability Density Functions

The random matrix's probability density function ([7]) is written as

If **A** is an  $n \times m$  real random matrix, then the matrix-variate probability density function of  $\mathbf{A} \in \mathbb{R}^{n \times m}$ , is represented  $p_{\mathbf{A}}(\mathbf{A})$ , is a mapping from the space of  $n \times m$  real matrices to the real line, i.e.,  $p_{\mathbf{A}}(\mathbf{A}) : \mathbb{R}^{n \times m} \to \mathbb{R}$ .

Below is the probability density functions of random matrices which are relevant to stochastic mechanics problems within this paper.

Wishart matrix: A  $n \times n$  symmetric positive definite random matrix **S** is known to have a Wishart distribution with parameters  $p \ge n$  and  $\Sigma \in \mathbb{R}_n^+$ , if its pdf is given by

$$p_{\mathbf{S}}(\mathbf{S}) = \left\{ 2^{\frac{1}{2}np} \Gamma_n \left( \frac{1}{2}p \right) \det \left\{ \Sigma \right\}^{\frac{1}{2}p} \right\}^{-1} |\mathbf{S}|^{\frac{1}{2}(p-n-1)} \operatorname{etr} \left\{ -\frac{1}{2} \Sigma^{-1} \mathbf{S} \right\}$$
(1)

This distribution is usually denoted as  $S \sim W_n(p, \Sigma)$ .

*Matrix variate Gamma distribution*: A  $n \times n$  symmetric positive definite random matrix **W** is said to have a matrix variate Gamma distribution with parameters a and  $\Psi \in \mathbb{R}_n^+$ , if its pdf is given by

$$p_{\mathbf{W}}(\mathbf{W}) = \{\Gamma_n(a) \det\{\mathbf{\Psi}\}^{-a}\}^{-1} \det\{\mathbf{W}\}^{a-\frac{1}{2}(n+1)} \exp\{-\mathbf{\Psi}\mathbf{W}\}; \quad \Re(a) > \frac{1}{2}(n-1)$$
 (2)

This distribution is usually denoted as  $\mathbf{W} \sim G_n(a, \Psi)$ . used the matrix variate Gamma distribution citesoi00 for the random system matrices for linear dynamical systems.

In Eqs. (1) and (2), the function  $\Gamma_n(a)$  is the multivariate Gamma function, this is represented as follows in terms of the univariate Gamma function products:

$$\Gamma_n(a) = \pi^{\frac{1}{4}n(n-1)} \prod_{k=1}^n \Gamma\left[a - \frac{1}{2}(k-1)\right]; \quad \text{for} \quad \Re(a) > \frac{1}{2}(n-1)$$
(3)

To obtain further information on matrix variate distributions, see [8, 7] and their corresponding references. The distributions provided by Eqs. (1) and (2) will always produce symmetric and positive definite matrices among the four types of random matrices discussed previously. As a result, they could be appropriate choices to represent random system matrices that emerge in probabilistic structural dynamics.

## 2.2 Probability density functions of the system matrices

In this section, we use the maximum entropy principle to obtain the probability density functions of the system matrices [9, 10]. Suppose that the mean values of  $\mathbf{M}$ ,  $\mathbf{C}$  and  $\mathbf{K}$  are given by  $\bar{\mathbf{M}}$ ,  $\bar{\mathbf{C}}$  and  $\bar{\mathbf{K}}$ , respectively. The random system matrices' matrix variate distributions should be such that

- (a) M, C and K are symmetric matrices,
- (b) M is positive-definite and C and K are non-negative-definite matrices, and
- (c) the moments of the dynamic stiffness matrix's inverse

$$\mathbf{D}(\omega) = -\omega^2 \mathbf{M} + i\omega \mathbf{C} + \mathbf{K} \tag{4}$$

should exist  $\forall \omega$ . That is, if the frequency response function (FRF) matrix,  $\mathbf{H}(\omega)$  is given by

$$\mathbf{H}(\omega) = \mathbf{D}^{-1}(\omega) = \left[ -\omega^2 \mathbf{M} + i\omega \mathbf{C} + \mathbf{K} \right]^{-1}$$
 (5)

then the following conditions must be satisfied:

$$\mathbb{E}\left[\|\mathbf{H}(\omega)\|_{\mathsf{F}}^{\nu}\right] < \infty, \quad \forall \, \omega \tag{6}$$

Here  $\nu$  is the order of the inverse-moment constraint.

If the matrix variate density function of  $\mathbf{G} \in \mathbb{R}_n^+$  is given by  $p_{\mathbf{G}}(\mathbf{G}) : \mathbb{R}_n^+ \to \mathbb{R}$ . We have the following information and constraints to obtain  $p_{\mathbf{G}}(\mathbf{G})$ :

$$\int_{\mathbf{G}>0} p_{\mathbf{G}}(\mathbf{G}) d\mathbf{G} = 1 \quad \text{(the normalization)}$$
 (7)

and 
$$\mathbb{E}[\mathbf{G}] = \int_{\mathbf{G}>0} \mathbf{G} \, p_{\mathbf{G}}(\mathbf{G}) \, d\mathbf{G} = \bar{\mathbf{G}}$$
 (the mean matrix) (8)

The integrals appearing in these equations are n(n+1)/2 dimensional, and the mean matrix  $\hat{\mathbf{G}}$  is symmetric and positive definite.

Maximising the entropy associated with the matrix variate probability density function  $p_{\mathbf{G}}(\mathbf{G})$ 

$$S(p_{\mathbf{G}}) = -\int_{\mathbf{G}>0} p_{\mathbf{G}}(\mathbf{G}) \ln \{p_{\mathbf{G}}(\mathbf{G})\} d\mathbf{G}$$
(9)

and using the constraints in Eqs. (7) and (8), it can be shown that [10] the maximum-entropy pdf of  ${\bf G}$  follows the Wishart distribution with parameters  $p=(2\nu+n+1)$  and  ${\bf \Sigma}=\bar{{\bf G}}/(2\nu+n+1)$ , that is  ${\bf G}\sim W_n\left(2\nu+n+1,\bar{{\bf G}}/(2\nu+n+1)\right)$ . The The maximum-entropy approach also gives the system parameters. The use of the Wishart distribution in structural dynamics has been studied for example in the books [11, 7]. introduced this measure of uncertainty citesoi00 as the dispersion parameter.

$$\mathbb{E}\left[\|\mathbf{G} - \mathbb{E}\left[\mathbf{G}\right]\|_{\mathsf{F}}^{2}\right] = \mathbb{E}\left[\operatorname{Trace}\left(\left[\mathbf{G} - \mathbb{E}\left[\mathbf{G}\right]\right]\left[\mathbf{G} - \mathbb{E}\left[\mathbf{G}\right]\right]^{\mathsf{T}}\right)\right]$$

$$= \operatorname{Trace}\left(\mathbb{E}\left[\mathbf{G}^{2}\right] - \mathbb{E}\left[\mathbf{G}\right]^{2}\right)$$

$$= \operatorname{Trace}\left(p\Sigma^{2} + p\operatorname{Trace}\left(\Sigma\right)\Sigma + p^{2}\Sigma^{2} - (p\Sigma)^{2}\right)$$

$$= p\operatorname{Trace}\left(\Sigma^{2}\right) + p\{\operatorname{Trace}\left(\Sigma\right)\}^{2}$$
(10)

Therefore

$$\delta_G^2 = \frac{p \operatorname{Trace}(\mathbf{\Sigma}^2) + p \{\operatorname{Trace}(\mathbf{\Sigma})\}^2}{p^2 \operatorname{Trace}(\mathbf{\Sigma}^2)} = \frac{1}{p} \left[ 1 + \frac{\{\operatorname{Trace}(\mathbf{\Sigma})\}^2}{\operatorname{Trace}(\mathbf{\Sigma}^2)} \right]$$
$$= \frac{1}{\theta + n + 1} \left[ 1 + \frac{\{\operatorname{Trace}(\bar{\mathbf{G}})\}^2}{\operatorname{Trace}(\bar{\mathbf{G}}^2)} \right]$$
(11)

Additionally, it has been demonstrated that in [12]  $\delta_G^2$  can be deduced using dispersion parameters of the mass and stiffness matrices. The deterministic (unreduced) system matrices  $\bar{\mathbf{G}}^{(i)} \equiv \{\bar{\mathbf{M}}^{(i)}, \bar{\mathbf{C}}^{(i)}, \bar{\mathbf{K}}^{(i)}\}$  of individual sub-components are required to generate the parameters of the Wishart random matrices, where the superscript (i) represent the system matrices of the  $i^{\text{th}}$  sub-component. To select the parameters p and  $\Sigma$  of the Wishart matrices, the criterion based on the optimal Wishart distribution has been adopted [10]. In this case, the deterministic matrix and its inverse are most equivalent to the means of the random matrix and its inverse. Mathematically, this implies  $\|\bar{\mathbf{G}} - \mathbb{E}[\mathbf{G}]\|_{\mathbf{F}}$  and  $\|\bar{\mathbf{G}}^{-1} - \mathbb{E}[\mathbf{G}^{-1}]\|_{\mathbf{F}}$  are minimum. This condition results in

$$p = n + 1 + \theta$$
 and  $\Sigma = \bar{\mathbf{G}}/\alpha$  (12)

where *n* is the size of  $\bar{\mathbf{G}}$ ,  $\alpha = \sqrt{\theta(n+1+\theta)}$  and  $\theta$  can be obtained as follows by using Eq. (11)

$$\theta = \frac{1}{\delta_G^2} \left[ 1 + \frac{\{\text{Trace}(\bar{\mathbf{G}})\}^2}{\text{Trace}(\bar{\mathbf{G}}^2)} \right] - (n+1)$$
 (13)

This method is justified because a random system matrix and its inverse are symmetric; positive-definite matrices should be treated mathematically similarly.

## 3. Methodology

# 3.1 The generalised Wishart random matrix model

The equation of motion of a damped n-degree-of-freedom linear dynamic system can be expressed as

$$\mathbf{M\ddot{q}}(t) + \mathbf{C\dot{q}}(t) + \mathbf{Kq}(t) = \mathbf{f}(t)$$
(14)

where  $\mathbf{f}(t) \in \mathbb{R}^n$  is the forcing vector,  $\mathbf{q}(t) \in \mathbb{R}^n$  is the response vector and  $\mathbf{M} \in \mathbb{R}^{n \times n}$ ,  $\mathbf{C} \in \mathbb{R}^{n \times n}$  and  $\mathbf{K} \in \mathbb{R}^{n \times n}$  are the mass, damping and stiffness matrices respectively. The dispersion parameter, proposed by Soize [9, 13], is a measure of uncertainty in the system, and it is similar to the normalised standard deviation of a matrix. For example, the dispersion parameter associated with the stiffness matrix is defined as

$$\delta_K^2 = \frac{\mathbb{E}\{\|\mathbf{K} - \mathbf{K}_0\|_{\mathrm{F}}^2\}}{\|\mathbf{K}_0\|_{\mathrm{F}}^2}$$
 (15)

where  $\|\cdot\|_F$  denotes the Frobenius norm of a matrix, and the symbol  $\mathbb{E}\{...\}$  denotes the operation of averaging to the corresponding probability distribution. The dispersion parameter  $\delta_M$  associated with the mass matrix can be defined similarly. The dispersion parameters  $\delta_M$  and  $\delta_K$  can be obtained using the stochastic finite element method or experimental measurements [14]. Given the dispersion parameters,  $\delta_M$  and  $\delta_K$  and the baseline mass and stiffness matrices  $\mathbf{M}_0$  and  $\mathbf{K}_0$ , the parameters for the random matrices  $\mathbf{M}$  and  $\mathbf{K}$  can be obtained in closed-form.

The dynamic matrix's eigensolutions describe the dynamic response of a proportionately damped stochastic system:

$$\mathbf{H} = \mathbf{M}^{-1/2} \mathbf{K} \mathbf{M}^{-1/2}. \tag{16}$$

It was shown that

$$\mathbf{H} \sim W_n\left(p, \Sigma\right) \tag{17}$$

where  $W_n(\bullet)$  denotes a n dimensional Wishart matrix. The parameters p and  $\Sigma$  can be obtained from the available data regarding the system, namely  $\mathbf{M}_0$ ,  $\mathbf{K}_0$ ,  $\delta_M$ , and  $\delta_K$ . Dynamical responses obtained using this generalised Wishart matrix have been validated [15] against the stochastic finite element method, full Wishart matrices and experiential results.

When Laplace transform is used on the equation of motion and assuming that all of the starting conditions are zero, (14), we have

$$[s^2\mathbf{M} + s\mathbf{C} + \mathbf{K}]\bar{\mathbf{q}}(s) = \bar{\mathbf{f}}(s)$$
(18)

where the Laplace transform of the respective quantities is denoted by  $(\bar{\bullet})$ . The statistical properties of  $\bar{\mathbf{q}}(s) \in \mathbb{C}^n$  when the system matrices are random matrices are obtained next. The undamped eigenvalue problem is thus written as

$$\mathbf{K}\phi_j = \omega_j^2 \mathbf{M}\phi_j, \quad j = 1, 2, \dots, n$$
 (19)

where  $\omega_j^2$  and  $\phi_j$  are, respectively, the eigenvalues and mass-normalised eigenvectors of the system. A high-resolution model of a dynamical system can easily have several million degrees of freedom (that is n). On the other hand, only a few hundred or thousands of modes may be necessary for calculating the dynamic response within the frequency range considered. Suppose the number of modes to be retained is m. In general,  $m \ll n$ . The selection of reduced modes depends on the frequency of excitation. If the maximum frequency of excitation is  $\omega_{\max}$ , then m should be such that at

least  $\omega_m > \omega_{\text{max}}$ . Several excellent references exist [16] on the selection of modal order for dynamic problems.

We form the truncated undamped modal matrices

$$\Omega = \text{diag}\left[\omega_1, \omega_2, \dots, \omega_m\right] \in \mathbb{R}^{m \times m} \quad \text{and} \quad \Phi = \left[\phi_1, \phi_2, \dots, \phi_m\right] \in \mathbb{R}^{n \times m}$$
 (20)

so that

$$\Phi^T \mathbf{K} \Phi = \Omega^2 \quad \text{and} \quad \Phi^T \mathbf{M} \Phi = \mathbf{I}_m$$
 (21)

where  $I_m$  is a m-dimensional identity matrix. Using the Eq. (18) can be transformed into the modal coordinates as

$$\left[s^2 \mathbf{I}_m + s \mathbf{C}' + \Omega^2\right] \bar{\mathbf{q}}' = \bar{\mathbf{f}}' \tag{22}$$

where and (•)' denotes the quantities in the reduced modal coordinates:

$$\mathbf{C}' = \Phi^T \mathbf{C} \Phi \in \mathbb{R}^{m \times m}, \quad \bar{\mathbf{q}} = \Phi \bar{\mathbf{q}}' \quad \text{and} \quad \bar{\mathbf{f}}' = \Phi^T \bar{\mathbf{f}}$$
 (23)

For simplicity, let us assume that the system is proportionally damped with deterministic modal damping factors  $\zeta_1, \zeta_2, \ldots, \zeta_m$ . Therefore, when we consider random systems, the matrix of eigenvalues  $\Omega^2$  in equation (22) will be a random matrix of dimension m. Suppose this random matrix is denoted by  $\Xi \in \mathbb{R}^{m \times m}$ :

$$\Omega^2 \sim \Xi$$
 (24)

From the definition of **H** in Eq. (5), it is clear that  $\Xi$  is a Wishart matrix, and the dispersion parameters of  $\Xi$  and **H** are the same. Since  $\Xi$  is a symmetric and positive definite matrix, it can be diagonalised by an orthogonal matrix  $\Psi_r$  such that

$$\Psi_r^T \Xi \Psi_r = \Omega_r^2 \tag{25}$$

In this case, the randomness of the eigenvalues and eigenvectors of the random matrix  $\Xi$  is denoted by the subscript r. Recalling that  $\Psi_r^T \Psi_r = \mathbf{I}_m$ , from equation (22) we obtain

$$\bar{\mathbf{q}}' = \left[ s^2 \mathbf{I}_m + s \mathbf{C}' + \Omega^2 \right]^{-1} \bar{\mathbf{f}}'$$
 (26)

$$= \Psi_r \left[ s^2 \mathbf{I}_m + 2s\zeta \Omega_r + \Omega_r^2 \right]^{-1} \Psi_r^T \mathbf{\bar{f}}'$$
 (27)

where

$$\zeta = \operatorname{diag}\left[\zeta_1, \zeta_2, \dots, \zeta_m\right] \in \mathbb{R}^{m \times m} \tag{28}$$

The original coordinate yielded the following response

$$\begin{split} \bar{\mathbf{q}}(s) &= \Phi \bar{\mathbf{q}}'(s) = \Phi \Psi_r \left[ s^2 \mathbf{I}_m + 2s \zeta \Omega_r + \Omega_r^2 \right]^{-1} (\Phi \Psi_r)^T \bar{\mathbf{f}}(s) \\ &= \sum_{j=1}^m \frac{\mathbf{x}_{r_j}^T \bar{\mathbf{f}}(s)}{s^2 + 2s \zeta_j \omega_{r_j} + \omega_{r_j}^2} \mathbf{x}_{r_j}. \end{split} \tag{29}$$

Here

$$\Omega_r = \operatorname{diag}\left[\omega_{r_1}, \omega_{r_2}, \dots, \omega_{r_m}\right] \tag{30}$$

and 
$$\mathbf{X}_r = \Phi \Psi_r = \begin{bmatrix} \mathbf{x}_{r_1}, \mathbf{x}_{r_2}, \dots, \mathbf{x}_{r_m} \end{bmatrix}$$
 (31)

are respectively the matrices containing random eigenvalues and eigenvectors of the system. The system's Frequency Response Function (FRF) can be obtained by substituting  $s = i\omega$  in Eq. (29). The computational methodology relies on the undamped random eigenvalue problems. Therefore, if a perturbation type of approach is adopted (for example [17]), then the method can be extended to general nonproportional or non-viscously [18] damped systems with light damping. In the next section, we summarise the Monte Carlo Simulation (MCS) based computational approach from this analysis.

## 3.2 Summary of the computational approach

A step-by-step method for implementing the new computational approach in conjunction with any general-purpose finite element software is given below:

- 1. Form the deterministic mass and stiffness matrices  $\mathbf{M}_0$  and  $\mathbf{K}_0$  using the standard finite element method and the modal damping factors  $\zeta_j$ . Select the number of modes m < n. The number of modes to be retained, m, should be selected based on the excitation frequency.
- 2. Solve the deterministic undamped eigenvalue problem

$$\mathbf{K}_{0}\phi_{0j} = \omega_{0j}^{2} \mathbf{M}_{0}\phi_{0j}, \quad j = 1, 2, \dots, m$$
(32)

and create the matrix

$$\Phi_0 = \left[\phi_{0_1}, \phi_{0_2}, \dots, \phi_{0_m}\right] \in \mathbb{R}^{n \times m} \tag{33}$$

Calculate the ratio

$$\beta_H = \left(\sum_{j=1}^m \omega_{0_j}^2\right)^2 / \sum_{j=1}^m \omega_{0_j}^4 \tag{34}$$

- 3. Obtain the dispersion parameters  $\delta_M$  and  $\delta_K$  corresponding to the mass and stiffness matrices. This can be obtained from physical or computer experiments.
- 4. Obtain the dispersion parameter of the generalized Wishart matrix H in Eq (16) as [15]

$$\delta_{H} = \frac{\left(p_{M}^{2} + (p_{K} - 2 - 2n) p_{M} + (-n - 1) p_{K} + n^{2} + 1 + 2n\right) \beta_{H}}{p_{K} \left(-p_{M} + n\right) \left(-p_{M} + n + 3\right)} + \frac{p_{M}^{2} + (p_{K} - 2n) p_{M} + (1 - n) p_{K} - 1 + n^{2}}{p_{K} \left(-p_{M} + n\right) \left(-p_{M} + n + 3\right)}$$
(35)

where

$$p_M = \frac{1}{\delta_M^2} \left\{ 1 + \{ \text{Trace} \mathbf{M}_0 \}^2 / \text{Trace} \mathbf{M}_0^2 \right\}$$
 (36)

and 
$$p_K = \frac{1}{\delta_K^2} \left\{ 1 + \{ \text{Trace} \mathbf{K}_0 \}^2 / \text{Trace} \mathbf{K}_0^2 \right\}$$
 (37)

5. Calculate the parameters

$$\theta = \frac{(1+\beta_H)}{\delta_H^2} - (m+1)$$
 and  $p = [m+1+\theta]$  (38)

where p is approximated to the nearest integer of  $m+1+\theta$ .

6. Create an  $m \times p$  matrix **Y** such that

$$Y_{ij} = \omega_{0i} \widehat{Y}_{ij} / \sqrt{\theta}; \quad i = 1, 2, \dots, m; j = 1, 2, \dots, p$$
 (39)

where  $\widehat{Y}_{ij}$  are Gaussian random numbers with zero mean and unit standard deviation and are independent and identically distributed (i.i.d.).

7. Simulate the  $m \times m$  Wishart random matrix

$$\Xi = \mathbf{YY}^T$$
 or  $\Xi_{ij} = \frac{\omega_{0_i} \omega_{0_j}}{\theta} \sum_{k=1}^{p} \widehat{Y}_{ik} \widehat{Y}_{jk}; \quad i = 1, 2, ..., m; j = 1, 2, ..., m$  (40)

Since  $\Xi$  is symmetric, only the upper or lower triangular part must be simulated.

8. Solve the symmetric eigenvalue problem  $(\Omega_r, \Psi_r \in \mathbb{R}^{m \times m})$  for every sample

$$\Xi \Psi_r = \Omega_r^2 \Psi_r \tag{41}$$

and obtain the random eigenvector matrix

$$\mathbf{X}_r = \Phi_0 \Psi_r = \left[ \mathbf{x}_{r_1}, \mathbf{x}_{r_2}, \dots, \mathbf{x}_{r_m} \right] \in \mathbb{R}^{n \times m}$$
(42)

9. Lastly, determine the frequency domain dynamic response as

$$\bar{\mathbf{q}}_r(i\omega) = \sum_{j=1}^m \frac{\mathbf{x}_{r_j}^T \bar{\mathbf{f}}(s)}{-\omega^2 + 2i\omega\zeta_j\omega_{r_j} + \omega_{r_j}^2} \mathbf{x}_{r_j}$$
(43)

Random eigensolutions can also provide time-domain response samples as

$$\mathbf{q}_{r}(t) = \sum_{j=1}^{m} a_{r_{j}}(t) \mathbf{x}_{r_{j}}, \text{ where } a_{r_{j}}(t) = \frac{1}{\omega_{r_{j}}} \int_{0}^{t} \mathbf{x}_{r_{j}}^{T} \mathbf{f}(\tau) e^{-\zeta_{j} \omega_{r_{j}}(t-\tau)} \sin\left(\omega_{r_{j}}(t-\tau)\right) d\tau$$
(44)

When using this method in conjunction with general-purpose commercial finite element software, the commercial program only has to be used once to retrieve the mean matrices  $\mathbf{M}_0$  and  $\mathbf{K}_0$  and solve the accompanying deterministic eigenvalue problem. Therefore, the computational procedure proposed here is 'nonintrusive'.

The main computationally intensive part of a random matrix-based approach is the generation of the random matrices (by matrix multiplication in Eq. (40)) and the solution of the eigenvalue problem. The matrix multiplication and the matrix eigenvalue problem scales approximately cubically with the dimension [19]. Therefore, the computational cost of the approach grows  $\approx O(m^3)$  compared to  $\approx O(n^3)$  for the full Wishart matrix-based approach. Since  $m \ll n$ , the reduced approach is expected to be computationally efficient.

## 3.3 Uncertainty quantification by unifying random matrices and model reduction

The following three methods were previously proposed by S. Adhikari [20] for the randomisation of system matrices:

- Method 1 Mass and stiffness matrices are fully correlated Wishart matrices: For this case  $\mathbf{M} \sim W_n(p_M, \Sigma_M)$ ,  $\mathbf{K} \sim W_n(p_K, \Sigma_K)$  with  $\mathrm{E}\left[\mathbf{M}\right] = \mathbf{M}_0$  and  $\mathrm{E}\left[\mathbf{K}\right] = \mathbf{K}_0$ . This is similar to the approach proposed by [9, 13] (the original approach requires the simulation of Gamma matrices [7], which is computationally more expensive). This method requires the simulation of two  $n \times n$  fully correlated Wishart matrices and the solution of a  $n \times n$  generalised eigenvalue problem with two fully populated matrices. The computational cost of this approach is  $\approx 2O(n^3)$ .
- Method 2 Generalized Wishart Matrix [15]: For this case  $\Xi \sim W_n\left(p,\Omega_0^2/\theta\right)$  with  $\mathrm{E}\left[\Xi^{-1}\right] = \Omega_0^{-2}$  and  $\delta_\Xi = \delta_H$ . This requires the simulation of one  $n \times n$  uncorrelated Wishart matrix and the solution of an  $n \times n$  standard eigenvalue problem. The computational cost of this approach is  $\approx O(n^3)$ .
- Method 3 Reduced diagonal Wishart Matrix: For this case  $\widetilde{\Xi} \sim W_m \left( \widetilde{p}, \widetilde{\Omega}_0^2 / \theta \right)$  with  $\operatorname{E} \left[ \widetilde{\Xi}^{-1} \right] = \widetilde{\Omega}_0^{-2}$  and  $\delta_{\widetilde{\Xi}} = \delta_H$ . We used a tilde to differentiate from the previous case. This requires simulating one  $m \times m$  uncorrelated Wishart matrix and solving a  $m \times m$  standard eigenvalue problem. m can be significantly smaller than n for large complex systems. The computational cost of this approach is  $\approx O(m^3)$ .

The methods are listed in decreasing order of computational cost. In this paper, we are using Method 3 for ease of computation. The samples of Wishart random matrices  $W_n(p,\Sigma)$  can be generated using *numpy* in Python. It can handle fractional values of  $(n+1+\theta)$  to avoid the approximation to its nearest integer.

The process needs to be repeated for the mass, stiffness, and damping matrices to acquire the relevant response statistics. Each sample's equation of motion is then solved. It is thus evident that this process is simple to follow. After the generation of system matrix samples, the remainder of the analysis is the same as that of any Monte Carlo simulation (MCS) based method. At this point, the mean matrices can be extracted using NASTRAN, which is accessed just once. Consequently, this simulation process is "nonintrusive." To analyse stochastic structures, a combined model reduction-based domain decomposition technique [12, 6] can simulate system random matrices efficiently. In this paper, however, we simplify the problem and utilise the generalised stiffness or eigenvalues generated from a free vibration analysis in Nastran to create our system matrix. We use the eigenvalues to create a diagonal matrix representing our generalised stiffness matrix. This method, however, denies us information regarding the dispersion parameters of the relevant system matrices. A numerical formulation is necessary for this; however, here, we use experimental observation and comparison of a few relevant  $\delta_H$  values to observe the variations. The next section explains a stepwise description of how this randomisation is carried out.

## 3.4 Parameter selection for Eigenvalue Analysis

There's a need to choose the free vibration analysis parameters to define the type of matrices utilised for the analysis. The options include:

• **Linear**: This default setting within Nastran applies the linear elastic stiffness matrix  $K_{AAX}$ , which assumes that the material behaviour is linearly elastic and the stiffness properties remain constant throughout the analysis. The eigenproblem corresponding to this stiffness matrix is given by:

$$\mathbf{K}_{AAX}\phi = \omega^2 \mathbf{M}\phi \tag{45}$$

• **Nonlinear**: This option utilizes the tangential stiffness matrix  $K_T$  derived from a previously executed nonlinear analysis. By assuming a linear mass matrix M and taking into account harmonic motion around quasi-static equilibrium states, the corresponding eigenproblem is provided. [21]:

$$\mathbf{K}_T \phi = \omega^2 \mathbf{M} \phi \tag{46}$$

This approach is beneficial when dealing with nonlinear material behaviour or large deformations. Note that tangential stiffness matrices are only constructed when the nonlinear analysis employs a Newton-Raphson iteration method. Other iteration methods, such as Constant Stiffness, Linear stiffness, or the secant (Quasi-Newton) method, do not construct tangent stiffness matrices. It was demonstrated that in the situation of small displacements and linear nature in pre-buckling, the sum of the geometric (prestress) contribution  $K_{GG}$  and the linear stiffness  $K_{AAX}$  may be approximated as the tangent stiffness. And the geometric (prestress) contribution [21].

• Geometric stress-stiffness: This parameter adds the geometric stress-stiffness matrix  $K_{GG}$  to the stiffness matrix K. This matrix accounts for the geometric nonlinearity arising from large displacements or rotations. The associated eigenproblem is:

$$(\mathbf{K} + \mathbf{K}_{GG})\phi = \lambda \mathbf{I}\phi \tag{47}$$

where  ${\bf K}$  is the symmetric stiffness matrix,  ${\bf M}$  is the mass matrix,  $\omega$  is the circular natural frequency,  $\lambda$  is the eigenvalue, and  $\phi$  is the mode shape vector or the related amplitude eigenvector. The eigenvalue  $\lambda$  equals  $\omega^2$ , which means the squared natural frequency in radians per second is equivalent to the eigenvalue. The eigenvector  $\phi$  represents the mode shape vector corresponding to this eigenvalue. Instead of extracting extensive stiffness matrix data, the analysis at this juncture uses a diagonal eigenvalue matrix as an alternative to the stiffness matrix. This approach primarily illustrates the variations in eigenvalues, representing the frequency ranges of different mode shapes from a free vibration analysis.

#### 4. Numerical illustration

## 4.1 Simple beam model

We start with a simple beam model for free vibration or eigenvalue analysis to simulate the proposed method. The nonlinear static analysis is intended to capture the model's response under applied loads, considering material nonlinearity and geometric complexities. The analysis is initiated with a multi-step nonlinear static SOL 400 command. Subsequently, a new subcase is initiated, consisting of two distinct steps. The first step involves a nonlinear static analysis under a designated load, followed by a normal modes analysis under the same load conditions. i.e., it begins with a load step of 5 kN and applies constraints to stabilise the model. Following this, to determine the natural frequencies and mode shapes of the structure a normal modes analysis is conducted. This analysis aids in understanding the dynamic behaviour of the model under free vibration conditions. The model consists of beam elements defined by grid points, with material properties specified for aluminium 1060 within the NASTRAN material library.

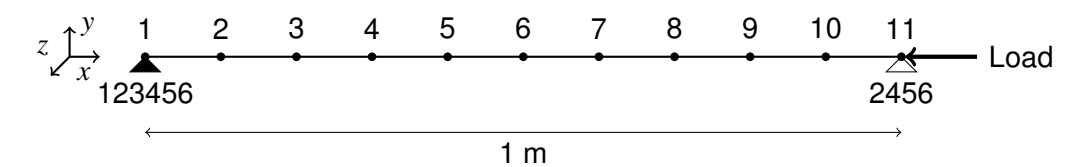


Figure 1 – Schematic diagram of the Nastran model of the simple beam structure. A fixed constraint (TX, TY, TZ, RX, RY & RZ fixed, i.e. 123456) at node one and pinned (TY, TZ, RY & RZ fixed, i.e. 2456 at node 11.)

The material selected for the analysis is Aluminum 1060 Annealed Wrought, characterised by a nominal density of  $2700~\text{kg/m}^3$ , an elastic modulus of 69~GPa, and a square cross-sectional width of 0.5~m. The material properties are defined using the MAT1 and MAT4 commands. The MAT1 command specifies an elastic modulus (E) and a Poisson's ratio  $\nu$  of 0.3~for isotropic materials, while the MAT4 command provides density  $\rho$ 

Boundary conditions are defined using the SPC1 command. Node 1 is fully constrained (123456), which means TX, TY, TZ, RX, RY & RZ fixed, where T & R denote translational and rotational degree of freedom, respectively, and node 11 has translational degrees of freedom in the Y and Z directions and all rotational degrees of freedom constrained (2456). Loadings are specified with the FORCE command, applying compressive force in the X direction at node 11.

Finally, the analysis is done to get the eigenvalues and eigenvectors for different loading conditions, allowing us to see the variation of mode shapes around the buckling load.

Next, the system is considered stochastic with no probabilistic description of the parameter variabilities. Hence, the system matrices are modelled as Wishart random matrices, and the response statistics are computed.

## 4.2 Scaling the technique to complex model

Here, we utilise a finite element model of a reinforced composite panel of aeronautical interest discussed in the previous work done by Pedro et al.[21] where experimental observations are made for the vibration correlation of this prestressed laminated reinforced panel. The FE model of the structure has 53188 nodes and 40823 elements. A visual depiction of the finite element model is displayed in (Fig 2) as visualised from a NASTRAN bulk data file. The AS4 unidirectional prepreg employed during the manufacturing of the reinforced composite panel has the following material properties:  $E_1 = 119$  GPa,  $E_2 = 9.8$  GPa,  $E_3 = 4.67$  GPa,  $e_{12} = 0.316$ ,  $e_{13} = 0.026$ ,  $e_{13} = 0.33$ ,  $e_{12} = 4.7$ GPa,  $e_{13} = 6.026$ ,  $e_{13} = 1.76$  GPa, and  $e_{15} = 1.580$  kg/m³. The manufacturer is Delft Aerospace Structures and Materials Laboratory[21].

Figure 3a illustrates the geometrical characteristics and boundary constraints used to generate the mathematical model. The two-stringer reinforced panel is 690mm long and b=270mm wide. Figure 3b depicts the dimensions of the cross-section. The stringer height and thickness are h=39.3mm and t=7.3mm, respectively, with  $h_1$ =9.52mm and  $h_2$ =3.66mm. Boundary conditions are applied to

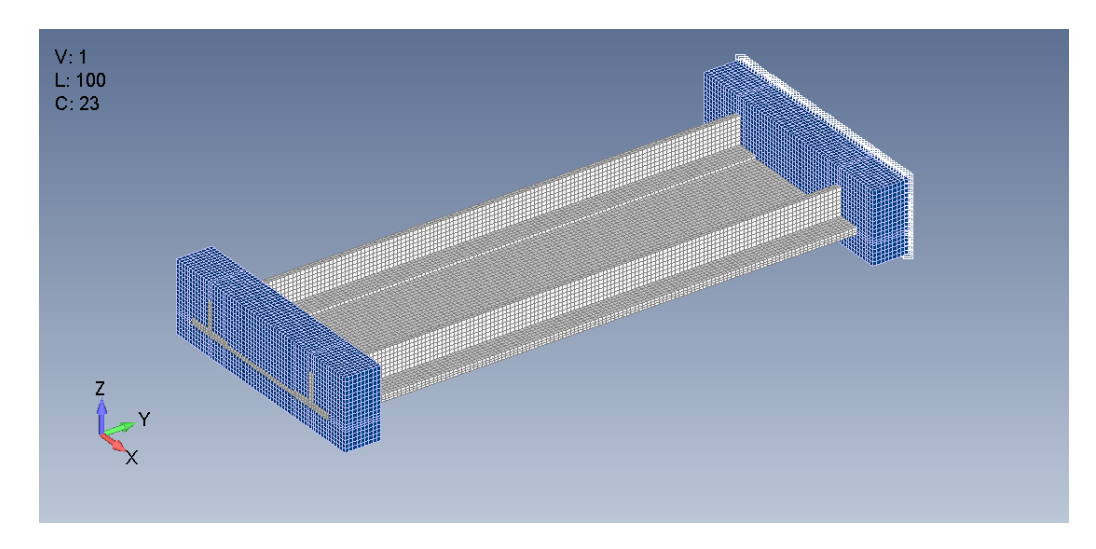


Figure 2 – FE model of the of the reinforced composite panel.

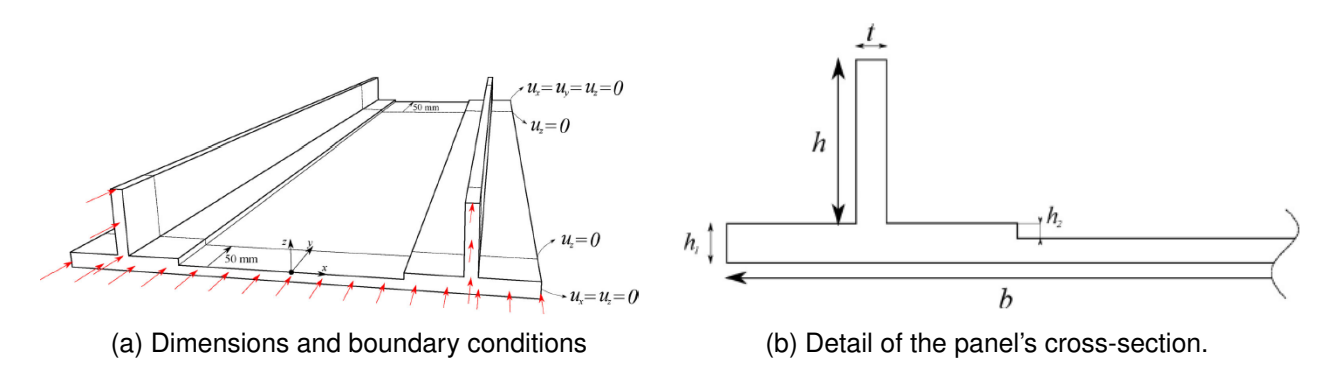


Figure 3 – Main geometrical features, loading and boundary conditions for the simulation of the reinforced composite panel.

displacement components on planes perpendicular to the y-axis, as seen in 3a. Two 50mm rigid bands are modelled at panel ends to simulate the effects of resin blocks. At y = 0, the cross-section is free to translate, yet pressure is applied to the whole plane[21].

The structure will be subjected to a prestressed nonlinear modal analysis to obtain the natural mode shapes [21], and the eigenvalue outputs are generated for 100 modes. This is done to compare the validity of the beam model and to verify the subsequent results from randomisation. The NASTRAN input file sets up a detailed structural analysis for a reinforced panel, encompassing nonlinear static and modal analyses. In the input file, the material properties are specified using NASTRAN's parameter settings, which include settings for large strain effects and shear transformations. The structural analysis, thus, considers nonlinearities and uses the RIKS method for the static step, suitable for post-buckling or large deformation problems. For the dynamic step, a complex eigenvalue extraction method METHOD = 100 is used to determine the natural frequencies and mode shapes.

Coordinate systems are defined using CORD2R entries, representing various stringer locations and base properties. These coordinate systems define local axes or reference frames for specific structural components, defining element orientations and material directions.

Boundary conditions are applied using SPC sets, with node constraints specified to restrict necessary translational and rotational degrees of freedom (TX, TY, TZ, RX, RY, RZ). Loadings are defined using FORCE and LOAD sets.

The analysis is set up to obtain the eigenvalues and eigenvectors within the  $. \pm 0.6$  file. Alternatively, output can also be obtained in .op2 or .op4 files. In this case, PyNastran can be used to read these files. This is done for multiple loading conditions to get the required data.

At this juncture, one may extract the relevant system matrices using DMAP (Direct Matrix Abstraction Program) commands within the bulk data file input. However, for a complex structure like this one,

the file size would be huge to process, so as a simpler method, we use eigenvalues, as they can be easily retrieved from the output files. The idea is to make the process computationally efficient and easy to perform.

#### 5. Results

The vibration correlation of the natural mode shapes from the simulation of the beam model and the reinforced panel is reviewed after the finite element analysis to verify the analogous characteristics of both models. Previous studies have carried out deterministic and experimental analyses to show the variation of the natural frequencies [21]. Here, we create a random profile for the eigenvalues (eigenvalue  $\lambda$  is equal to  $\omega^2$ , the squared natural frequency in radians per second) for different modes using our Wishart random matrix model. The process begins with creating a fully populated Wishart random matrix from the diagonal eigenvalue matrix ( $\lambda$ I). NASTRAN was employed for the preliminary analysis to obtain the eigenvalues that need to be randomised. The eigenvalues are stored as a diagonal matrix and follow the numerical steps mentioned in 3.2 to generate the Wishart matrices, following which Monte-Carlo simulation is performed to generate an ensemble of multiple Wishart matrices. To handle extensive data, a sparse matrix format is used for large Wishart matrices to reduce memory usage.

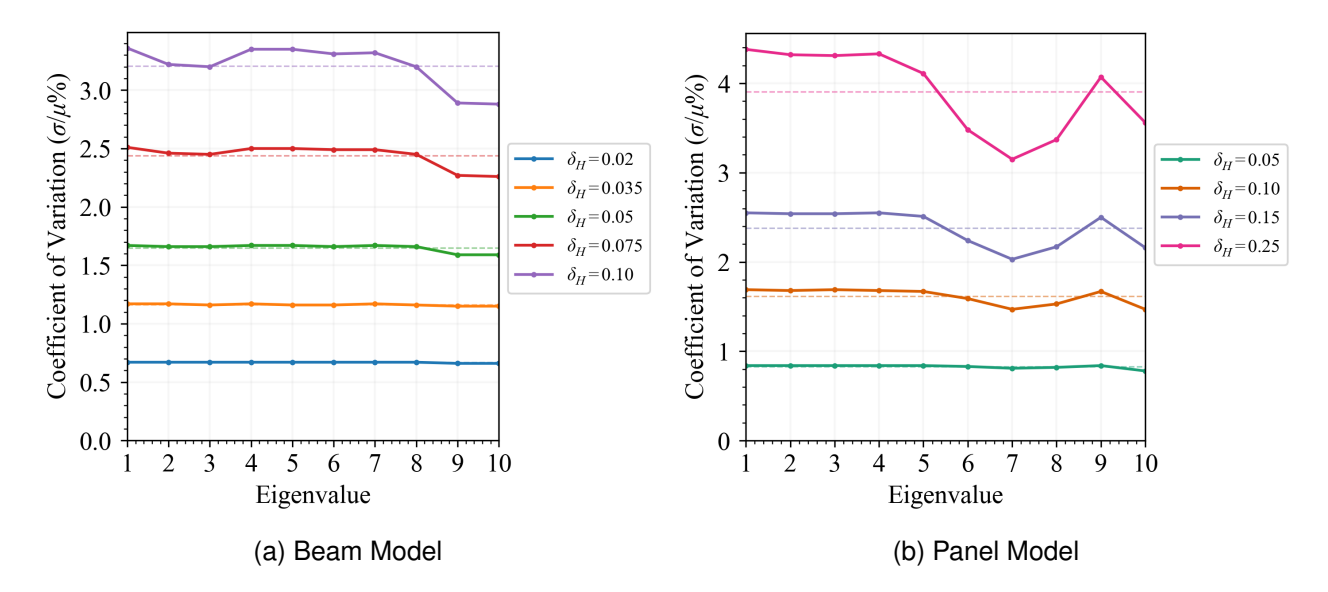


Figure 4 – Coefficient of variation of randomised eigenvalues for different values of dispersion parameter  $\delta_H$  across the first 10 Eigenvalue index from 100,000 MCS

## 5.1 Dispersion Parameter

Adjustments to the dispersion parameter  $\delta_H$  and the size of the Wishart matrix are required to ascertain the extent of variation and establish the appropriate tolerance for uncertainty. The size of the Wishart matrix is typically determined by the input matrix, which may consist of the stiffness matrix or, in our scenario, the diagonal eigenvalue matrix. Since we opted for eigenvalues and considering that free vibration analysis may theoretically yield infinite eigenvalues—albeit with diminishing significance for higher ones—we can select the necessary number to construct the Wishart matrix. However, suppose the stiffness matrix, dictated by the structure and contingent upon the number of elements in the finite element model, is employed, the size of the Wishart matrix remains constant. In this study, we used the first 100 modes of the complex panel model and 38 modes from the simple beam model (due to design limitations, geometric restrictions and coarse meshing, it did not yield more eigenvalues for this particular analysis, which was done deliberately to understand the variations in less defined models).

The dispersion parameters are analysed for both models to check for the Coefficient of Variation (CoV) across the first ten eigenvalue indices. This can be compared with experimental observation to decide the required  $\delta_H$  value to be utilised for the prediction. However, in the absence of experimental

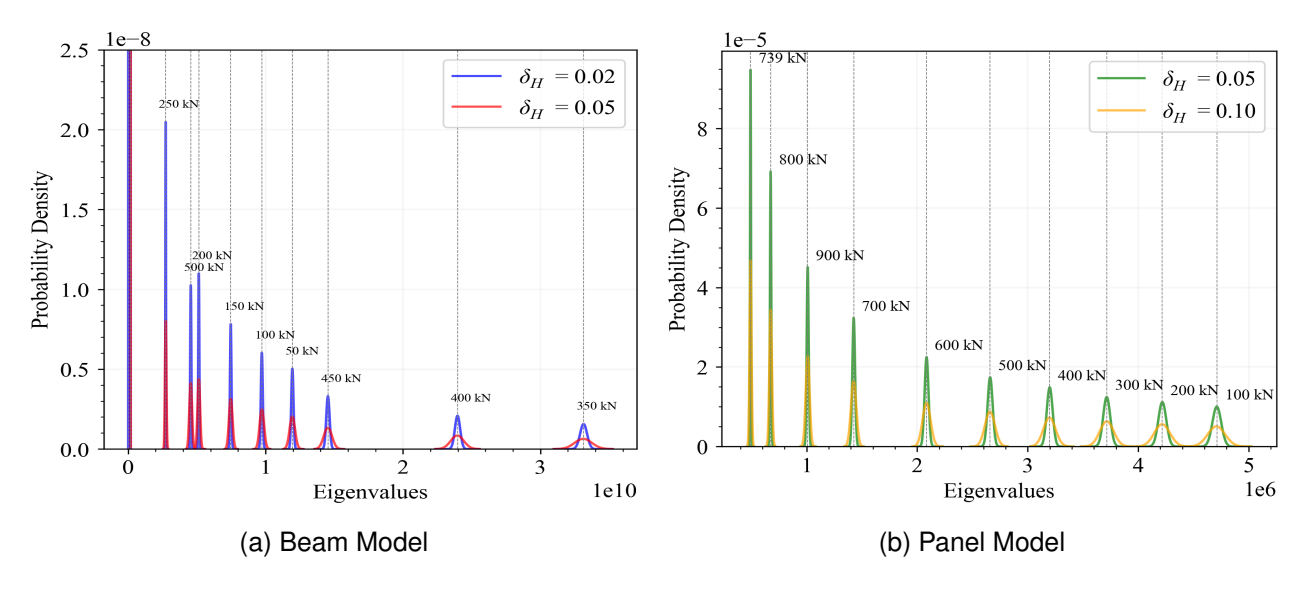


Figure 5 – Probability Density Function plot of different  $\delta_H$  for Eigenvalue 1 across different loading values for a single loading value

data to validate the range of dispersion as well as the lack of information without explicitly investigating the individual dispersion parameters of the mass and stiffness matrix of the finite element models, we resort to a careful consideration based on the convergence and low value of per cent coefficient of variation(CoV%), preferably below one. So, we analyse a particular loading condition to check for the variation for 100,000 Monte-Carlo Samples(MCS) of Wishart randomised eigenvalue matrices and the results are presented in figure 4. Higher values above unit per cent CoV are improbable in this case, however, we analyse them to see the behaviour of the dispersion parameter. As we can see from the figure, the higher CoVs become unpredictable even for higher Monte Carlo simulations. Also, we can see that the unpredictability increases for higher eigenmodes. Finally, we choose  $\delta_H = 0.02$  for the simple beam model, which converges to a CoV = 0.67 and for the complex panel model,  $\delta_H = 0.05$  which converges to CoV = 0.84.

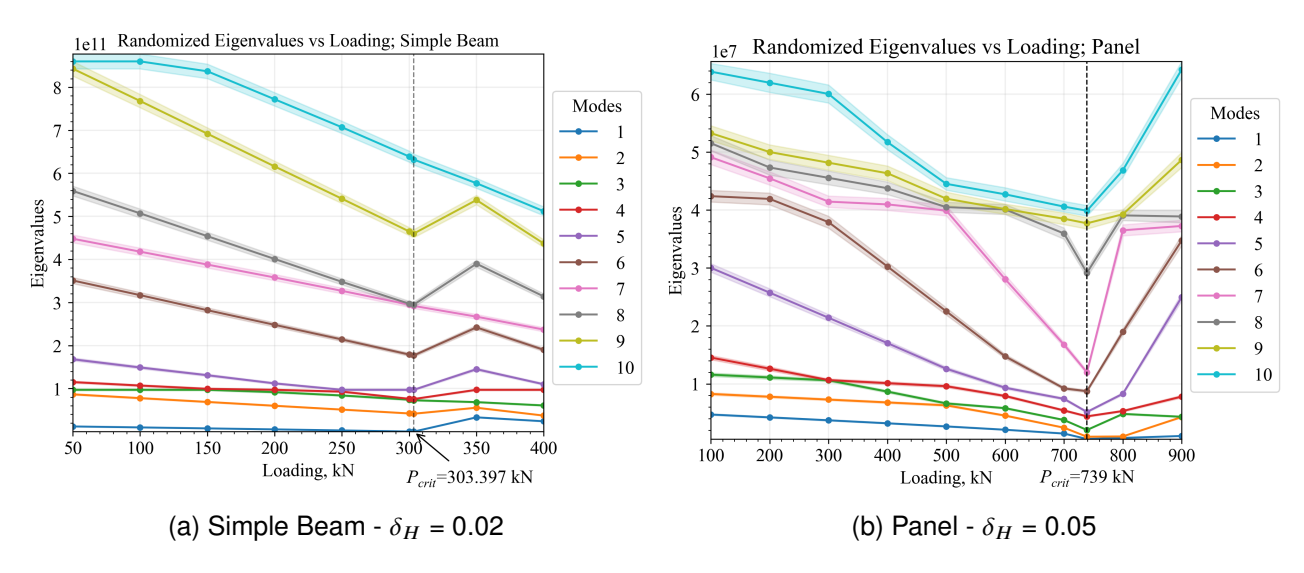


Figure 6 – Randomized Eigenvalues across Loading; within three standard deviations of the PDF, first ten modes

To comprehend the practical meaning of changes in the dispersion parameter, we display a graph depicting the variation in probability density for two different  $\delta_H$  values for each model under different loading conditions. This graph is presented in figure 5. As discussed earlier, the CoV% converges to the same value across the different loading conditions. Here, the significant change occurs with the standard deviation. The deviation is much leaner closer to the critical buckling load and is the

lowest at the critical buckling load, suggesting the least variation. Overall, this observation signifies that as the dispersion parameter is allowed to increase, the bandwidth of frequencies for a particular mode increases, leading to more uncertainty, which may be useful in situations that demand a wide margin of safety. With a low dispersion parameter value, this uncertainty is much more localised. However, the lowest permissible value of  $\delta_H$  should be analysed based on an experimental result or an expected theoretical outcome. As this method can be utilised for other analyses, one has to critically examine the underlying physics to choose the required dispersion based on the spread, which can be done through a few experimental and theoretical validation processes.

## 5.2 Plotting the randomized eigenvalues

The shaded plot provides a visual representation of the variability or uncertainty around the eigenvalue loci at each point along the loading for the vibration correlation results for the simple beam and panel model. The shaded plots are plotted for the dispersion parameter,  $\delta_H=0.02$  for the simple beam and  $\delta_H=0.05$  for the panel model as discussed in the previous section 5.1 In this case, the shaded area is created around the main line plot (the eigenvalues) within three standard deviations of the probability distribution of each eigenvalue. The lower boundary is calculated by subtracting the standard deviation from the main line, and the upper boundary is calculated by adding the standard deviation to the main line.

As the CoV remains the same, the standard deviation is higher for higher modes, and thus, the spread may not be visible for lower modes when more modes are displayed on a single plot, as we have shown the first ten modes for both the models in figure 6. Hence, an additional plot for clarity is shown for the first four modes in figure 7.

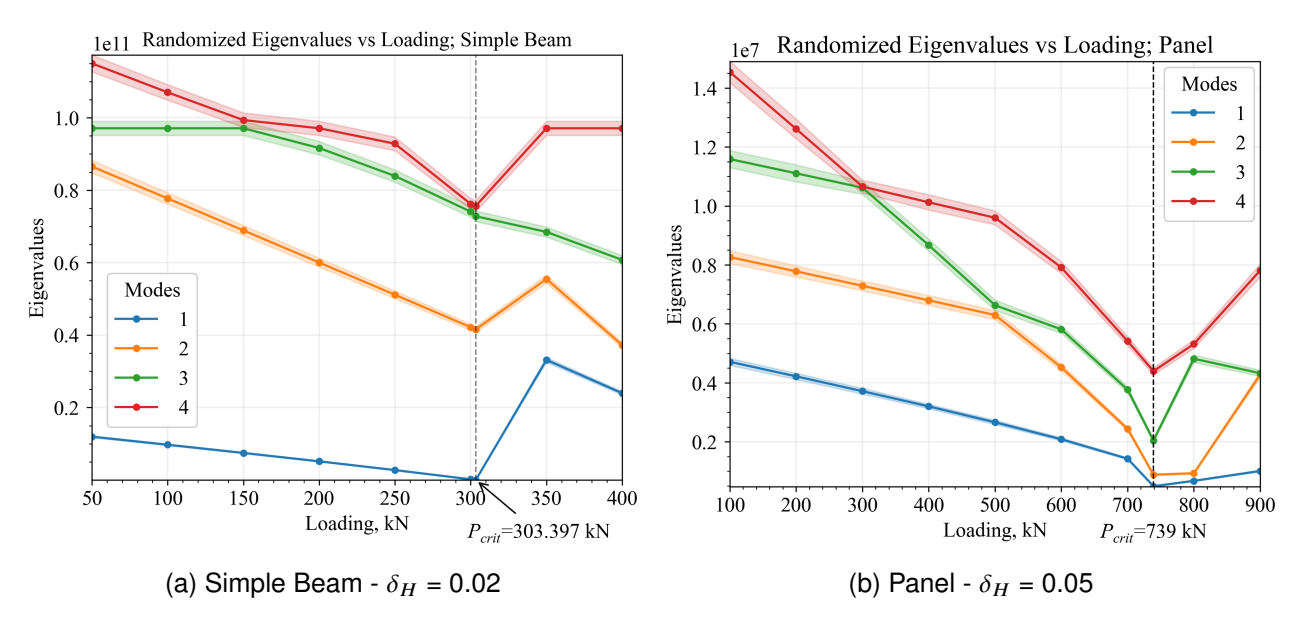


Figure 7 – Randomized Eigenvalues across Loading; within three standard deviations of the PDF, first four modes

#### 5.3 Discussions

An approximation is made in choosing the relevant dispersion parameter based on the convergence of the CoV%, which requires a mathematical validation as a new system parameter is utilised, i.e., the eigenvalues, instead of the characteristic stiffness or mass matrix, which has a defined dispersion parameter derived using the Frobenius norm of the matrix. In the shaded plots of the eigenvalue loci, there are few instances of very close occurrences of these loci, which can be seen to cross or veer suddenly away from each other, called mode veering, for a detailed discussion about this phenomenon we may refer [22, 23, 24, 25, 26, 27]. Although, within the deterministic results the modes do not overlap, the shaded plot has an overlap observed, which needs further investigation. Figure 8 shows a closer look at these instances. As this needs a more rigorous investigation, a

detailed explanation of the order of modes of the randomised values cannot be explicitly stated within the domains of this study.

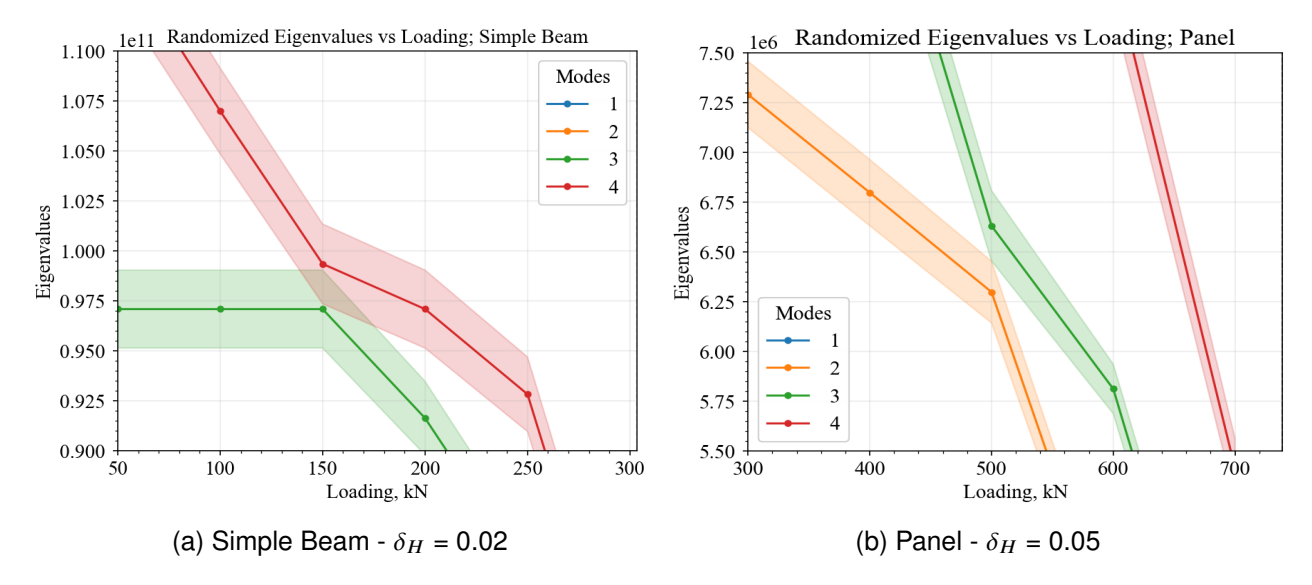


Figure 8 – A closer look into the close occurrences of eigenvalue loci within the shaded plot of randomised eigenvalues for simple beam and panel model

In low-frequency vibration scenarios, the probability distributions of individual eigenvalues provide significant physical insights when the matrix size and uncertainties are limited. However, in random systems with variable parameters, phenomena such as the veering effect and statistical overlap of eigenvalues become prominent [28]. The veering effect describes the crossing or mixing of eigenvalues as system parameters change. At the same time, statistical overlap occurs when the eigenvalues start to merge, particularly for higher eigenvalues of large matrices or systems with significant uncertainties [29]. It was shown that even for moderately uncertain systems with  $\delta_k^2 = 0.25$ , substantial statistical overlap can occur with as few as 30 eigenvalues [30]. When modes exhibit veering and substantial statistical overlap is present, the physical relevance of the probability distribution of individual ordered eigenvalues becomes questionable. Traditional perturbation-based methods may appear less valid in these scenarios, especially when the standard deviation of the eigenvalues exceeds the mean spacing between them [17, 31]. In such situations, an alternative approach that considers the density of a collection of eigenvalues proves more meaningful [32, 33, 34]. This density-based approach becomes particularly relevant for aerospace structures like helicopters and spacecraft, which frequently experience high-frequency vibrations that can excite numerous higher modes.

The code we developed for this numerical method uses a sparse matrix format to reduce memory and computing time; however, the process remains computationally demanding when considering systems of higher scales, such as an entire aircraft. Hence, further optimisation is essential to accommodate larger matrix sizes. This can be achieved using parallel computing significantly enhancing performance and scalability. Essential strategies that may be employed include domain decomposition, which allows the issue to be split up and tackled in parallel, and effective load balancing, which distributes the computing burden equally. Additionally, leveraging high-performance computing (HPC) frameworks and libraries optimised for sparse matrix operations, such as PETSc [35]or Trilinos [36], can provide substantial improvements. Implementing these strategies may not only accelerate the computation but also enable handling more complex models and higher resolution simulations, thus extending the applicability of the sparse matrix approach to large-scale engineering problems like aircraft structural analysis, which can be a scope for further study.

### 6. Conclusions

In this paper, using the Wishart random matrix model, a simplified eigenvalue randomisation technique is presented as a viable and cost-effective means of analysing prestressed vibration correlation studies in structures of aeronautical importance without precise knowledge of the uncertainty. The

dynamic stiffness matrix changes with the force term in a prestressed condition. To represent this change, we use the diagonal eigenvalue matrix from a natural frequency analysis with geometric prestress, which is randomised using Wishart matrices. The variation is studied, and the results are stated.

- 1. In prestressed structures, the dynamic stiffness matrix differs from non-stressed structures, introducing additional considerations for the analysis.
- 2. The absence of a requirement for explicit information regarding joint uncertainty remains advantageous, as quantifying joint uncertainties in prestressed structures can be particularly intricate.
- 3. Computational efficiency is maintained in prestressed systems through diagonal eigenvalue matrix to create random matrices and employing sparse matrix format.
- 4. Parallel computations in the Monte Carlo Simulation (MCS) framework persist, allowing for efficient analysis of prestressed structures.
- The generalised nature of the approach extends seamlessly to prestressed structures, accommodating different dynamic stiffness matrices and handling uncertainties in multi-component systems.
- 6. Additional considerations in uncertainty modelling may arise due to the influence of prestress, and the framework can be adapted to address these specifics in the analysis.
- 7. Mode veering phenomena showed few statistical overlaps within the boundaries of consecutive mode loci and may need further investigation.

A few drawbacks of the proposed approach that demand further examination, particularly in the context of prestressed structures and complex systems with a large number of elements and degrees of freedom, are:

- It is crucial to determine the matrix variate joint probability density function for M,C, and K, particularly in light of the complex behaviour of large-scale structures and the complications brought about by prestress. Although using eigenvalues can make this process easier, it may also create more uncertainty if not modelled without proper considerations with the selection of parameters, which might be beneficial or detrimental, depending on the analysis's requirements.
- Handling the intricate interactions among numerous elements and degrees of freedom introduces complexities that need careful consideration in the modelling and analysis.
- Despite the use of sparse matrix format to reduce memory and computing time, the numerical
  method remains computationally demanding for larger systems such as entire aircraft, necessitating further optimisation through parallel computing and the implementation of HPC frameworks to handle complex models and high-resolution simulations, indicating a potential area for
  further research.

#### 7. Contact Author Email Address

mailto: a.mannoosseril.1@research.gla.ac.uk; sondipon.adhikari@glasgow.ac.uk

# 8. Copyright Statement

The authors confirm that they, and/or their company or organisation, hold copyright on all of the original material included in this paper. The authors also confirm that they have obtained permission from the copyright holder of any third-party material included in this paper to publish it as part of their paper. The authors confirm that they give permission, or have obtained permission from the copyright holder of this paper, for the publication and distribution of this paper as part of the ICAS proceedings or as individual off-prints from the proceedings.

#### References

- [1] R. Ghanem and P. D. Spanos. Stochastic Finite Elements: A Spectral Approach. Springer-Verlag, New York, USA, 1991.
- [2] A. Haldar and S. Mahadevan. Reliability Assessment Using Stochastic Finite Element Analysis. John Wiley and Sons, New York, USA, 2000.
- [3] S. Adhikari and S. Mukherjee. The exact element stiffness matrices of stochastically parametered beams. *Probabilistic Engineering Mechanics*, 69:103317, 2022.
- [4] Karl-Alexander Hoppe, Martin G. T. Kronthaler, Kian Sepahvand, and Steffen Marburg. Identification of a cantilever beam's spatially uncertain stiffness. *Scientific Reports*, 13(1), January 2023.
- [5] James Bergstra, Brent Komer, Chris Eliasmith, Dan Yamins, and David D Cox. Hyperopt: a python library for model selection and hyperparameter optimization. *Computational Science and Discovery*, 8(1):014008, jul 2015.
- [6] Tanmoy Chatterjee, Sondipon Adhikari, Michael Friswell, and Hamed Khodaparast. Non-parametric stochastic reduced-order modelling of built-up structures. In *Proceedings of International Conference on Noise and Vibration Engineering*, 09 2022.
- [7] A.K. Gupta and D.K. Nagar. *Matrix Variate Distributions*. Monographs & Surveys in Pure & Applied Mathematics. Chapman & Hall/CRC, London, 2000.
- [8] Antonia M. Tulino and Sergio Verdú. Random Matrix Theory and Wireless Communications. now Publishers Inc., Hanover, MA, USA, 2004.
- [9] C. Soize. A nonparametric model of random uncertainties for reduced matrix models in structural dynamics. *Probabilistic Engineering Mechanics*, 15(3):277–294, 2000.
- [10] S. Adhikari. Wishart random matrices in probabilistic structural mechanics. *ASCE Journal of Engineering Mechanics*, 134(12):1029–1044, December 2008.
- [11] R. J. Muirhead. Aspects of Multivariate Statistical Theory. John Wiely and Sons, New York, USA, 1982.
- [12] S. Adhikari and R. Chowdhury. A reduced-order non-intrusive approach for stochastic structural dynamics. *Computers and Structures*, 88(21-22):1230–1238, 2010.
- [13] C. Soize. Maximum entropy approach for modeling random uncertainties in transient elastodynamics. *Journal of the Acoustical Society of America*, 109(5):1979–1996, May 2001. Part 1.
- [14] M. Arnst, D. Clouteau, H. Chebli, R. Othman, and G. Degrande. A non-parametric probabilistic model for ground-borne vibrations in buildings. *Probabilistic Engineering Mechanics*, 21(1):18–34, 2006.
- [15] S. Adhikari. Generalized wishart distribution for probabilistic structural dynamics. *Computational Mechanics*, 45(5):495–511, May 2010.
- [16] D. J. Ewins. *Modal Testing: Theory and Practice*. Research Studies Press, Baldock, England, second edition, 2000.
- [17] S. Adhikari. Rates of change of eigenvalues and eigenvectors in damped dynamic systems. *AIAA Journal*, 37(11):1452–1458, November 1999.
- [18] S. Adhikari. Eigenrelations for non-viscously damped systems. *AIAA Journal*, 39(8):1624–1630, August 2001.
- [19] J. H. Wilkinson. The Algebraic Eigenvalue Problem. Oxford University Press, Oxford, UK, 1988.
- [20] S. Adhikari and R. Chowdhury. A reduced-order random matrix approach for stochastic structural dynamics. Computers & Structures, 88(21–22):1230–1238, Nov 2010.
- [21] Pedro H. Cabral, Erasmo Carrera, Henrique E. A. A. dos Santos, Pedro H. G. Galeb, Alfonso Pagani, Daniel Peeters, and Alex P. Prado. Experimental and numerical vibration correlation of pre-stressed laminated reinforced panel. *Mechanics of Advanced Materials and Structures*, 29(15):2165–2175, 2022.
- [22] C. Pierre. Mode localization and eigenvalue loci veering phenomena in disordered structures. *Journal of Sound and Vibration*, 126(3):485–502, 1988.

- [23] Christophe Pierre and Raymond H Plaut. Curve veering and mode localization in a buckling problem. *Z. Angew. Math. Phys.*, 40(5):758–761, September 1989.
- [24] B.R. Mace1 and E. Manconi. Mode veering in weakly coupled systems. In *Proceedings of the International Conference on Noise and Vibration engineering*. ISMA, 2012.
- [25] J. L. du Bois, S. Adhikari, and N. A. J. Lieven. Mode veering in stressed framed structures. *Journal of Sound and Vibration*, 322(4-5):1117–1124, May 2009.
- [26] J. L. du Bois, S. Adhikari, and N. A. J. Lieven. An experimental and numerical investigation of mode veerings. In *Proceedings of the 25th International Modal Analysis Conference (IMAC-XXV)*, Orlando, Florida, USA, February 2007.
- [27] A. Gallina, L. Pichler, and T. Uhl. Enhanced meta-modelling technique for analysis of mode crossing, mode veering and mode coalescence in structural dynamics. *Mechanical Systems and Signal Processing*, 25(7):2297 – 2312, 2011.
- [28] J. L. du Bois, S. Adhikari, and N. A. J. Lieven. On the quantification of eigenvalue curve veering: A veering index. *Transactions of ASME, Journal of Applied Mechanics*, 78(4):041007:1–8, 2011.
- [29] C. S. Manohar and A. J. Keane. Statistics of energy flow in one dimentional subsystems. *Philosophical Transactions of Royal Society of London*, A346:525–542, 1994.
- [30] C. Soize. Random matrix theory and non-parametric model of random uncertainties in vibration analysis. Journal of Sound and Vibration, 263(4):893–916, 2003.
- [31] S. Adhikari. Calculation of derivative of complex modes using classical normal modes. *Computer and Structures*, 77(6):625–633, August 2000.
- [32] L. Pastur and M. Shcherbina. Eigenvalue Distribution of Large Random Matrices. American Mathematical Society, Providence, RI, USA, 2011.
- [33] Madan Lal Mehta. Random Matrices. Academic Press, San Diego, CA, second edition, 1991.
- [34] S. Adhikari, L. Pastur, A. Lytova, and J. L. Du-Bois. Eigenvalue-density of linear stochastic dynamical systems: A random matrix approach. *Journal of Sound and Vibration*, 331(5):1042–1058, 2012.
- [35] Satish Balay, William D. Gropp, Lois Curfman McInnes, and Barry F. Smith. *Efficient Management of Parallelism in Object-Oriented Numerical Software Libraries*, pages 163–202. Birkhäuser Boston, Boston, MA, 1997.
- [36] Michael A. Heroux, Roscoe A. Bartlett, Vicki E. Howle, Robert J. Hoekstra, Jonathan J. Hu, Tamara G. Kolda, Richard B. Lehoucq, Kevin R. Long, Roger P. Pawlowski, Eric T. Phipps, Andrew G. Salinger, Heidi K. Thornquist, Ray S. Tuminaro, James M. Willenbring, Alan Williams, and Kendall S. Stanley. An overview of the trilinos project. ACM Trans. Math. Softw., 31(3):397–423, sep 2005.

# 9. Appendices

# 9.1 Nastran Commands Mentioned in the paper

The following is a list of NASTRAN commands used in this paper, listed in order of usage.

Table 1 – List of NASTRAN commands used in the paper

Command	Description			
SOL 400	Specifies solution sequence and options for structural analysis using MSC Nastran solver			
MAT1	Defines material properties for linear isotropic materials			
MAT4	Defines material properties for linear orthotropic materials			
SPC1	Specifies single-point constraints (SPCs) to restrain degrees of freedom			
FORCE	Specifies concentrated force or moment loads			
RIKS	Sets up a Riks analysis for studying nonlinear behaviour			
METHOD = 100	Specifies numerical method for analysis			
CORD2R	Defines a rectangular Cartesian coordinate system			
SPC	Specifies constraints to restrict motion of degrees of freedom			
LOAD	Specifies applied loads, forces, moments, or temperatures			
.f06	Output file format for storing analysis results, readable text format			
.op2	Output file format for storing binary results data			
.op4	Output file format for storing binary results data			

# 9.2 Coefficient of Variation data of Randomized Eigenvalues

The tables below show the Coefficient of variation (CoV) of randomised eigenvalues for different dispersion parameter values  $\delta_H$  across the first 10 Eigenvalue index from 100,000 MCS for 100kN loading.

Table 2 – Comparison of CoV values for simple beam and panel models

(a)	) CoV	' values	for simp	le beam	model
-----	-------	----------	----------	---------	-------

(b) CoV values for panel model

$\delta_H$				$\delta_H$						
Eigenmode	0.02	0.035	0.05	0.075	0.10	Eigenmode	0.05	0.10	0.15	0.25
1	0.67	1.17	1.67	2.51	3.36	1	0.84	1.69	2.55	4.38
2	0.67	1.17	1.66	2.46	3.22	2	0.84	1.68	2.54	4.32
3	0.67	1.16	1.66	2.45	3.2	3	0.84	1.69	2.54	4.31
4	0.67	1.17	1.67	2.5	3.35	4	0.84	1.68	2.55	4.33
5	0.67	1.16	1.67	2.5	3.35	5	0.84	1.67	2.51	4.11
6	0.67	1.16	1.66	2.49	3.31	6	0.83	1.59	2.24	3.48
7	0.67	1.17	1.67	2.49	3.32	7	0.81	1.47	2.03	3.15
8	0.67	1.16	1.66	2.45	3.2	8	0.82	1.53	2.17	3.37
9	0.66	1.15	1.59	2.27	2.89	9	0.84	1.67	2.5	4.07
10	0.66	1.15	1.59	2.26	2.88	10	0.78	1.47	2.16	3.56

# 9.3 Probability Distribution Values for comparing dispersion parameter

Table 3 – Probability Density Function data for Eigenvalue 1 across different loading values for a single loading value for beam model

(a)  $\delta_H = 0.02$ 

(b)  $\delta_H = 0.05$ 

Load (kN)	CoV(%)	Max PDF	Load (kN)	CoV (%)	Max PDF
50	0.6633	$5.03 \times 10^{-9}$	50	1.6364	$2.04 \times 10^{-9}$
100	0.6786	$6.04 \times 10^{-9}$	100	1.6524	$2.48 \times 10^{-9}$
150	0.6829	$7.82 \times 10^{-9}$	150	1.7041	$3.14 \times 10^{-9}$
200	0.7031	$1.10 \times 10^{-8}$	200	1.7693	$4.38 \times 10^{-9}$
250	0.7127	$2.05 \times 10^{-8}$	250	1.8150	$8.03 \times 10^{-9}$
300	0.7463	$2.96 \times 10^{-7}$	300	1.8474	$1.19 \times 10^{-7}$
303.39	0.7391	$7.45 \times 10^{-3}$	303.39	1.8470	$2.98 \times 10^{-3}$
350	0.7673	$1.57 \times 10^{-9}$	350	1.8952	$6.36 \times 10^{-10}$
400	0.7973	$2.09 \times 10^{-9}$	400	1.9749	$8.43 \times 10^{-10}$
450	0.8287	$3.31 \times 10^{-9}$	450	2.0479	$1.34 \times 10^{-9}$
500	0.8531	$1.03 \times 10^{-8}$	500	2.1245	$4.12 \times 10^{-9}$

Table 4 – Probability Density Function data for Eigenvalue 1 across different loading values for a single loading value for panel model

(a)  $\delta_H = 0.05$ 

(b)  $\delta_H = 0.10$ 

Load (kN)	CoV(%)	Max PDF	Load (kN)	CoV (%)	Max PDF
100	0.8417	$1.01 \times 10^{-5}$	100	1.6703	$5.07 \times 10^{-6}$
200	0.8446	$1.12 \times 10^{-5}$	200	1.6851	$5.61 \times 10^{-6}$
300	0.8604	$1.25 \times 10^{-5}$	300	1.6997	$6.32 \times 10^{-6}$
400	0.8358	$1.10 \times 10^{-8}$	400	1.7156	$7.27 \times 10^{-6}$
500	0.8594	$1.49 \times 10^{-5}$	500	1.7112	$8.77 \times 10^{-6}$
600	0.8490	$1.74 \times 10^{-5}$	600	1.7421	$1.10 \times 10^{-5}$
700	0.8643	$2.25 \times 10^{-5}$	700	1.7035	$1.64 \times 10^{-5}$
739	0.8561	$3.24 \times 10^{-5}$	739	1.7341	$4.68 \times 10^{-5}$
800	0.8559	$9.48 \times 10^{-5}$	800	1.7179	$3.45 \times 10^{-5}$
900	0.8761	$4.51 \times 10^{-5}$	900	1.7432	$2.27 \times 10^{-5}$